

Systematic Multi-Parametric Analysis of Acute Myeloid Leukemia (AML) Flow Cytometry Drug Screens using Flowty

—Master Thesis—

Augusta Jensen

augustavangjensen@gmail.com

Supervisors: David Bryder and Krister Wennerberg
david.bryder@med.lu.se, krister.wennerberg@bric.ku.dk

Examiner: Magnus Carlquist
magnus.carlquist@tmb.lth.se

A collaboration between
Lund University and University of Copenhagen



LUND
UNIVERSITY



17 January 2023 - 7 June 2023
Copenhagen, Denmark

Abstract

English

Acute myeloid leukemia (AML) is a heterogeneous disease, making it difficult to treat. The standard treatment is intensive chemotherapy and has not changed in 40 years. However, recently new drugs and as less intensive treatment regimens have been approved in the US and in Europe. However. With a larger therapeutic toolbox, there is an urgent need for predictive biomarkers to offer the optimal treatment for the patient, also referred to as precision medicine. This project investigated AML flow cytometry drug screens using the unpublished analytical application, Flowty. Cellular subpopulations present in AML bone marrow samples were visualized based on their phenotypic expression of the biomarkers CD34, CD38, CD33, CD45, CD64, CD117 and HLA-DR, as well as granularity. This enabled investigation of whether AML patients and subpopulations with similar differentiation phenotypes have similar drug response. The aim was to explore the possibility of using differentiation phenotype to dictate on AML precision medicine. The heterogeneity in drug response was evident when comparing patients. However, exploring a small patient cohort, subpopulations with similar phenotypic expression demonstrated a similar drug response across patients. Furthermore, future aspects of research were proposed, focusing on additional analysis of the correlations between phenotypic expression and drug response.

Swedish

Akut myeloisk leukemi (AML) är en heterogen sjukdom, vilket gör den svår att behandla. Standardbehandlingen är intensiv kemoterapi och har inte förändrats på 40 år. På senare tid har nya läkemedel och mindre intensiva behandlingsregimer godkänts i USA och Europa. Fler möjliga behandlingsformer gör att det krävs prediktiva biomarkörer och tillförlitliga utvärderingsmetoder för att hitta den optimala behandlingen hos patienterna, så kallat precisionsmedicin. I detta projekt undersöktes flödescytometriska läkemedelsscreens för AML med hjälp av den opublicerade analytiska applikationen Flowty. Cellulära subpopulationer hos patienter med AML visualiserades baserat på deras fenotypiska uttryck av biomarkörerna CD34, CD38, CD33, CD45, CD64, CD117 och HLA-DR, samt granularitet. Detta gjorde det möjligt att undersöka huruvida AML-patienter och subpopulationer med liknande differentieringsfenotyper har liknande läkemedelsrespons. Syftet var att undersöka möjligheten att använda differentieringsfenotyper för att styra precisionsmedicin för AML. Heterogeniteten i läkemedelsresponsen var uppenbar när man jämförde mellan patienter. Subpopulationer med liknande fenotypiskt uttryck visade dock liknande läkemedelsrespons mellan patienter, vid undersökning av en liten patientgrupp. Vidare forskningsaspekter föreslogs, med fokus på ytterligare analys av sambandet mellan fenotypiskt uttryck och läkemedelsrespons.

Acknowledgment

This master's project was performed during spring 2023 in Krister Wennerberg's group at the Biotech Research & Innovation Center, BRIC, at the University of Copenhagen. The master's project is in collaboration with the Department of Applied Microbiology at the Faculty of Engineering, Lund University.

First, I would like to thank all my colleagues in the Wennerberg group for welcoming me into the team. A special thanks to Krister Wennerberg, my supervisor, for leading me along this project, supporting me with ideas and helping me to filter mutation data, and to Sarah Unterberger for all the lessons and support you shared with me along this project.

Thanks to David Bryder, for acting as my main supervisor at LU, enabling me to do this project and for the feedback along the way, and thanks to Magnus Carlquist for serving as my master's degree examiner.

I also want to acknowledge and thank Sandra Gordon, who was responsible for running the patient flow cytometry drug screens in the High-Throughput Translational Hematology (HTTH) facility, generating the data used in this project, and Mikhail Osipovitch, the developer of Flowty, for supporting me with ideas and information about Flowty. Thanks to Jakob Schmidt Jespersen, for sharing the patient DNA sequencing data, and to the artificial intelligence, ChatGPT (OpenAI, 2023), for teaching me about R programming and assisting me with R-programming scripts, which has been very useful throughout this project.

Contents

1	Introduction	4
2	Project Aim & Research Questions	4
3	Background	5
3.1	Myelopoiesis	5
3.2	Acute Myeloid Leukemia	6
3.2.1	Current Classification and Treatment of AML	6
4	Materials & Methods	8
4.1	Overall Workflow	8
4.2	Patient Samples	8
4.3	Flow Cytometry Drug Screening	9
4.4	Flowty Analysis	11
4.5	Data Analysis	14
5	Result & Discussion	15
5.1	Which Are the Least Differentiated Cells, and Their Phenotypes, in Each AML Patient?	15
5.1.1	Identifying and Characterizing Subpopulations	15
5.2	Do Similar Differentiating AML Patients Have Similar Drug Response?	19
5.2.1	Comparing Patients Based on Subpopulation Composition	19
5.2.2	Analyzing the Relationship Between Subpopulation Composition and Drug Response across Patients	21
5.3	Do Similar Subpopulations, Between Different AML Patients, Have Similar Drug Response?	24
5.3.1	Drug Response Analysis of Subpopulations across Multiple Patients	24
5.3.2	Drug Response Analysis of Subpopulations from Individual Flowty Runs	28
6	Future Aspects	33
7	Conclusion	33

1 Introduction

Acute myeloid leukemia (AML) is a blood cancer that is genetically and phenotypically heterogeneous [1]. It is one of the most common types of leukemia in adults, with an average age at diagnosis of 68 years [2]. The standard treatment has not changed in over 40 years, and the 5-year overall survival in Sweden is only 2% in patients diagnosed at the age of 70–89 years [3, 4]. Recently, several new drugs for treating AML patients have been approved in the US by the US Food and Drug Administration (FDA) and in Europe by the European Medicines Agency’s (EMA) [5]. Having a larger therapeutic toolbox allows for more opportunities, but also raises the challenge of finding the optimal treatment for each patient. To find new effective therapies, investigation of novel biomarkers that predict therapeutic response in patients is therefore of great interest [6].

In the last couple of decades, the characterization of AMLs has shifted from using morphological phenotypes, to almost exclusively, using genetic alterations as prognostic and predictive biomarkers [7]. However, single cell analytical tools, such as multi-parametric flow cytometry analyses, have evolved and greatly improved the phenotypic characterization of AMLs [8].

This provides the opportunity to explore AML cell phenotypes and the differentiation hierarchies of AML as new or additional biomarkers guiding therapy. However, traditional manual gating of cellular subpopulations in scatter plots, where you look at two biomarkers at a time, is inefficient. Finding new, unexpected, subpopulations is also challenging using this method [9]. New ways to analyze these high-dimensional data is therefore needed. One example of such is *FlowSOM*, a visualization technique, which uses clustering algorithms to identify cell subpopulations [10].

2 Project Aim & Research Questions

The aim of this master’s project was to systematically analyze multiparametric flow cytometry drug screening data from AML patients in order to characterize the phenotypic expression and answer the following research questions:

Which are the least differentiated cells, and their phenotypes, in each AML patient?

Do similar differentiating AML patients have similar drug response?

Do similar subpopulations, between different AML patients, have similar drug response?

The purpose of addressing these research questions is to investigate whether the differentiation phenotype could be used to dictate AML precision medicine. The project also contributes to the development of ”Flowty”, an unpublished bioinformatic analytical application, by showing its practical usage.

3 Background

3.1 Myelopoiesis

In our bone marrow, we have hematopoietic stem cells (HSC) that have the ability to self-renew and differentiate into all the different cells in our blood. During the differentiation, the cells gain molecular functions and lose their self-renewal ability. Fluorochrome labelled antibodies and flow cytometry made it possible to study and characterize the cell types formed during the hematopoietic differentiation, also known as hematopoiesis. This approach is useful to study hematological disorders [11].

Initially, HSCs embark on a path of differentiation, leading them to become multipotent progenitors (MPPs). These MPPs differentiate into lymphoid-primed multipotent progenitors (LMPPs) and common myeloid progenitors (CMPs). These progenitors give rise to two primary branches known as the lymphoid and myeloid arms. Simplified, the lymphoid arm consists of LMPPs that through a common lymphoid progenitor differentiate into mature lymphocytes, such as T cells, B cells, natural killer cells, and dendritic cells. In the myeloid arm, common myeloid progenitors (CMPs) give rise to two distinct lineages: granulocyte/macrophage lineage-restricted progenitors (GMPs) and megakaryocyte/erythrocyte lineage-restricted progenitors (MEPs). LMPPs have the potential to form GMPs, but not MEPs. Through several intermediate stages, these progenitors ultimately differentiate into various mature cell types such as granulocytes, dendritic cells, macrophages, platelets, and erythrocytes [11, 12].

Figure 1 illustrates the myeloid arm, which is also referred to as myelopoiesis. Furthermore, the figure depicts the expression of specific cell surface markers, including CD34, CD38, CD33, CD45, CD64, CD117, and HLA-DR, which aid in identifying and distinguishing cell types [11, 13]. Primarily, these markers differentiate cell types within the granulocyte and monocyte lineages. Acute myeloid leukemia can emerge at any of these cellular stages, except for the end stages of myelopoiesis that typically have restricted proliferative activity [14].

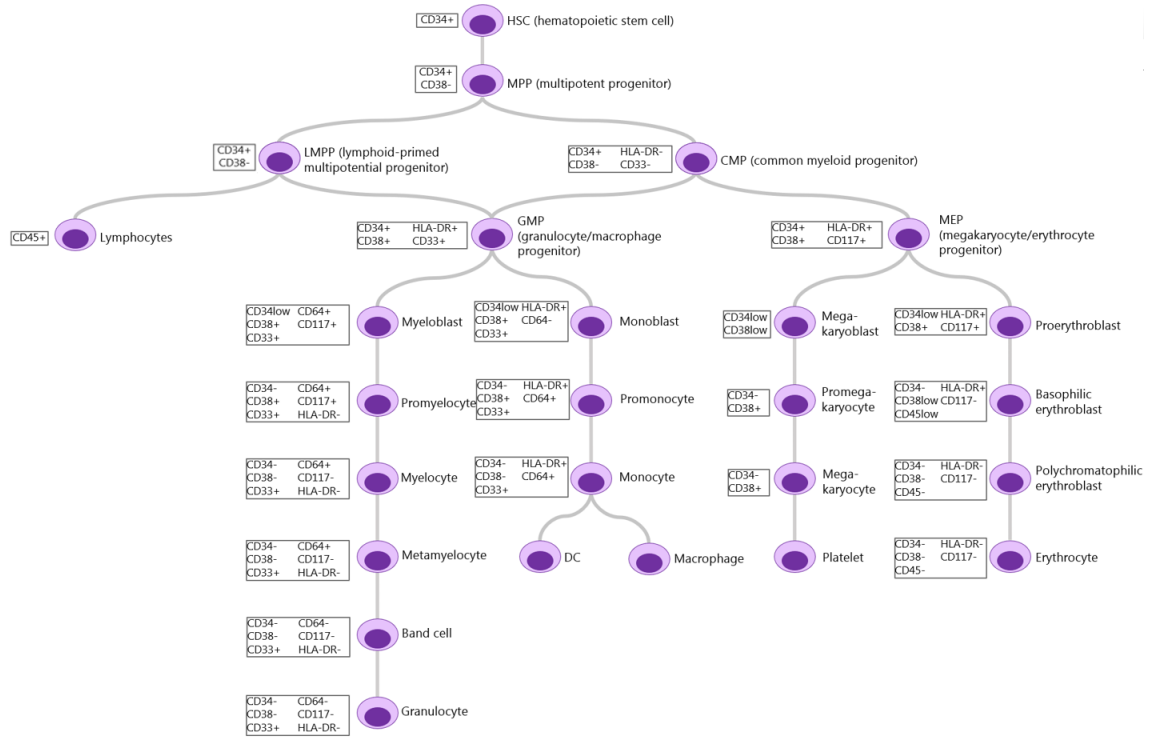


Figure 1. Illustration of the myelopoiesis. The expressions of the biomarkers *CD34*, *CD38*, *CD33*, *CD45*, *CD64*, *CD117* and *HLA-DR* are shown for each cell type. (Adapted from [11, 12, 13])

3.2 Acute Myeloid Leukemia

AML, or acute myeloid leukemia, is an oncogenic hematopoietic disorder characterized by the clonal expansion of myeloid stem cells and progenitor cells within the bone marrow. This abnormal proliferation leads to the formation of leukemic blasts, which are aberrant blood cells that disrupt the normal process of myelopoiesis [14].

Among adults, AML is one of the most common types of leukemia. The median age at diagnosis is 68 years [2]. The 5-year overall survival in Sweden and Denmark is 22% and 27%, respectively. However, for patients diagnosed at the age of 70–89 years, the 5-year overall survival in Sweden and Denmark is only 2% and 1%, respectively [4].

AML is an exceptionally complex and heterogeneous disease, most often arising from mutations in various leukemia-associated genes. Patients often have more than one driver mutation and the disease evolves over time with clones competing. The most common driver mutations are in the genes *NPM1*, *FLT3* and *CEBPA* [15]. Moreover, AML can also progress from other myeloid diseases, such as myelodysplastic syndrome. This type of AML is referred to as secondary and accounts for more than 25% of AML [16].

3.2.1 Current Classification and Treatment of AML

The heterogeneity within and between patients challenges the classification of AML. In 1976, the French American British (FAB) classification was first introduced [17]. It divides

AML into eight different subgroups (M0-M7) based on the cell morphology in the bone marrow [18]. The European LeukemiaNet (ELN) genetic classification (favorable, intermediate, and adverse) to predict clinical outcome is also widely used nowadays [19]. The state-of-the-art classification currently used to diagnose AML is the 2017 World Health Organization (WHO) Classification, which is based on genetics [20]. In the new 5th edition of WHO Classification, AML that were previously categorized as *not otherwise specified* due to lack of genetic abnormalities are now referred to as defined by differentiation [21].

The standard of care for AML patients has been induction chemotherapy with cytarabine and anthracycline, since the 1970s, and autologous stem cell transplantation (ASCT) since the 1980s, making it one of the few diseases with limited therapeutic advancements [3, 22]. However, the majority of AML patients are considered unfit for intensive chemotherapy and are instead treated with low-dose cytarabine (LDAC) and hypomethylating agents (HMAs), for example azacitidine. While these alternative treatments can extend survival, they do not offer curative outcomes [6]. Lately, there has been a remarkable advance in AML drug discovery, with 10 new approved drugs by the FDA, of which 7 have been approved in Europe by the EMA. However, predictive markers for these targeted therapies are mostly lacking [5].

In a recent study by Zeng et al., AML heterogeneity was investigated using transcriptomics data to determine cellular hierarchy composition and the association to therapy response. The findings suggest that biomarkers based on leukemia cell hierarchy composition hold promise for the development and selection of precision medicine approaches in AML [23]. This is the field where this project aims to contribute.

4 Materials & Methods

4.1 Overall Workflow

The overall workflow for this research project is illustrated in Figure 2. The first five steps describes the flow cytometry drug screening, which was performed prior to the start of this master’s project. This project starts with the Flowty analysis and the last step illustrates the main part of this master’s project, which involves creating and evaluating approached to address the research questions, using the Flowty outputs.

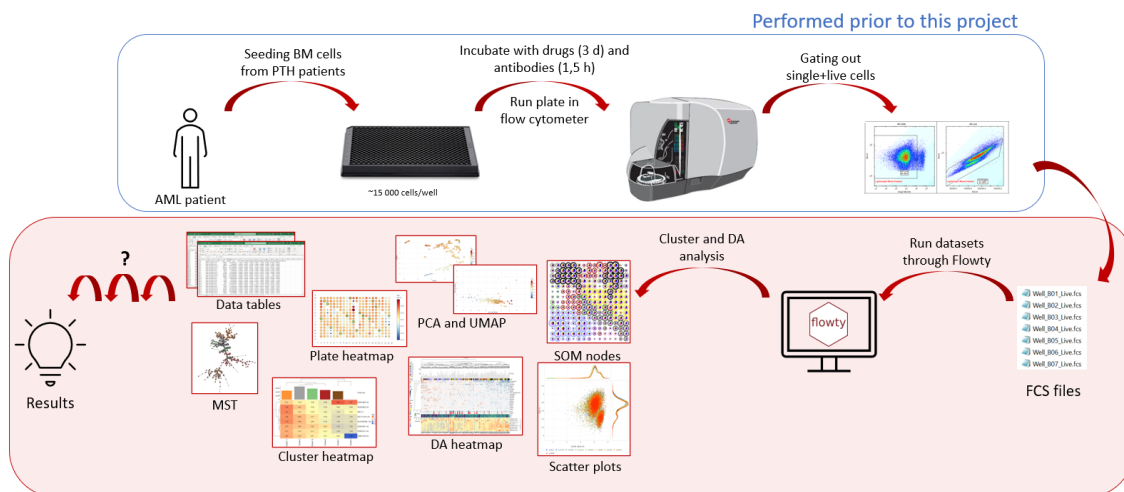


Figure 2. Schematic overview of the overall workflow. (1) Bone marrow sample from AML patient were seeded into a 384 well plate. (2) The cells were incubated with drugs (3 days) and antibodies (1,5 h) before the plate was run through the flow cytometer. (3) Live and dead cells were manually gated out in Forecyt. (4) Flow cytometry standard (FCS) files were extracted with information about the single and live cells of each well. (5) The FCS files were run through Flowty. (6) Flowty generates cluster and differential abundance analysis of the drug screen plate in the form of graphs, plots and data tables. (7) Methodologies used to address the research questions. The steps enclosed in red are the ones included in this project.

4.2 Patient Samples

Mononuclear cells were isolated from donated human bone marrow from 22 AML patients enrolled in the Program for Translational Hematology (PTH). Written informed consent was obtained from each patient according to the Danish National Ethical committee/National Videnskabetisk Komité (permit 1705391).

The patient information was gathered from RedCap. The average age at sample collection was 70 years and the cohort consists of 12 males and 10 females, primary ($n = 16$), secondary ($n = 5$) and one relapse patient. The patients are classified using the FAB classification, consisting of M0 ($n = 1$), M1 ($n = 4$), M2 ($n = 9$), M4 ($n = 6$) and M5 ($n = 2$), and the ELN risk classification, consisting of favorable ($n = 1$), intermediate ($n = 10$) and adverse ($n = 11$). DNA sequencing data was filtered to obtain the most likely driver mutations in each patient. The patient information is specified in Table 1.

Table 1. Patient Information. The hyphen (-) indicates missing data.

ID	Age	Gender	Type	Risk	FAB	Mutations
1	78	Male	Primary	Adverse	M2	BCOR, BCORL1, DNMT3A KRAS, NRAS, RUNX1 SETD2, U2AF1
2	48	Male	Primary	Favorable	M4	CEBPA, GATA2, NRAS
3	71	Male	Primary	Adverse	M4	ASXL2, FLT3, SUZ12 TP53
4	44	Male	Primary	Adverse	M1	NCOR2, PTPN11, TP53
5	76	Male	Secondary	Adverse	M2	FLT3, NPM1, TET2
6	70	Male	Primary	Intermediate	M2	CEBPA, STAG2
7	60	Male	Relapse	Adverse	M4	-
8	71	Female	Primary	Intermediate	M5	BRAF, DNMT3A, FLT3 NPM1, RUNX1, TET2 ZRSR2
9	70	Female	Primary	Intermediate	M2	-
10	77	Male	Primary	Intermediate	M0	-
11	74	Male	Primary	Intermediate	M2	CEBPA, IDH2, STAG2 WT1
12	78	Female	Secondary	Adverse	M2	ASXL1, IDH1, RUNX1 ZRSR2
13	61	Female	Primary	Adverse	M1	CUX1, NOTCH2, RUNX1
14	77	Female	Primary	Intermediate	M2	IDH2, NCOR2, RUNX1 SRSF2
15	73	Female	Primary	Adverse	M4	ASXL1, ATRX, RUNX1 SF3B1
16	92	Male	Primary	Intermediate	M5	ASXL1, EZH2, RUNX1
17	60	Male	Secondary	Adverse	M2	STAG2
18	71	Male	Secondary	Intermediate	M1	BRCC3, EP300, IDH2 SUZ12
19	40	Female	Secondary	Adverse	M1	GNAS, WT1
20	85	Female	Primary	Adverse	M4	BCOR
21	57	Female	Primary	Adverse	M4	-
22	77	Female	Primary	-	M1	-

4.3 Flow Cytometry Drug Screening

The bone marrow cells from patients were distributed into a 384-well plate, with an approximate seeding of 15,000 cells per well. Over a period of 72 hours, the cells were subjected to incubation with 40 drugs (Table 2) using a seven-point concentration range. Afterward, fluorescently labeled antibodies, which target seven specific biomarkers distinguishing different cellular subpopulations, along with Draq7, a DNA-binding dye for detecting dead cells, were introduced to the plate. The plate was then incubated for 1.5 hours before being analyzed using a high-throughput flow cytometer (iQue Screener Plus, Intellicyte). The antibody panel listed in Table 3 specifies the particular biomarkers employed in this experiment. After the flow cytometry, the data was manually gated to obtain live and single cells using the Draq7 and FSC.

Table 2. Drug panel. All drugs are used in a seven-point concentration gradient.

Drug Name	Drug Name
Dexamethasone	Tamibarotene
Methotrexate	Selinexor
Etoposide	Birabresib
Eprentapopt	Idasanutlin
Mitoxantrone	Enasidenib
Vincristine	Gilteritinib
Palbociclib	A-1331852
Navitoclax	Ivosidenib
Ponatinib	Tazemetostat
Trametinib	Idelalisib
BAY-2402234	A-366
ruxolitinib	Pyrrvinium pamoate
Dasatinib	YKL-06-062
Iadademstat	Azacitidine
Sorafenib	Venetoclax
NVP-MIK665	Combo Venetoclax/ azacitidine
Midostaurin	Daunorubicin
Onvansertib	Cytarabine
Copanlisib	Combo cytarabine/daunorubicin
Pevonedistat	
SNDX-5613	

Table 3. Antibody panel. The channel specifies the red (RL), violet (VL) and blue (BL) lasers and whether the height (H) or area (A) is detected.

Biomarker	Fluorophore	Clone	Ab Isotype	Vendor	Ref. No.	Lot No.	Detector
CD34	APC	563	IgG1	BD Bioscience	561209	0073826	RL1-H
CD38	BV421	HB7	IgG1	BioLegend	356618	B293282	VL1-H
CD45	PE-Cy7	HI30	IgG1	BioLegend	304016	B286744	BL5-H
CD117	BV605	104D2	IgG1	BD Bioscience	562687	0042133	VL4-H
HLA-DR	AF488	6H6	IgG2a	Biolegend	307620	B271228	BL1-H
CD33	PE	WM53	IgG1	BioLegend	303404	B314615	BL2-H
CD64	BV786	10,1	IgG1	BioLegend	305044	B284669	VL6-H
Draq7	APC-Cy7	-	-	Biolegend	424001	273DR71000	RL2-H

The flow cytometer measures the single cells as they are transported through a laser beam. The laser excites the fluorophores at a specific wavelength, and the fluorophores then emit light in another wavelength. The fluorescence emission light from the fluorophores are detected at approximately 90-degree angle of the beam. The side scatter (SSC) and the forward scatter (FCS) of the light is proportional to the granularity, or internal complexity, and the size of the cell respectively [24]. In Figure 3, the components of a flow cytometer are illustrated.

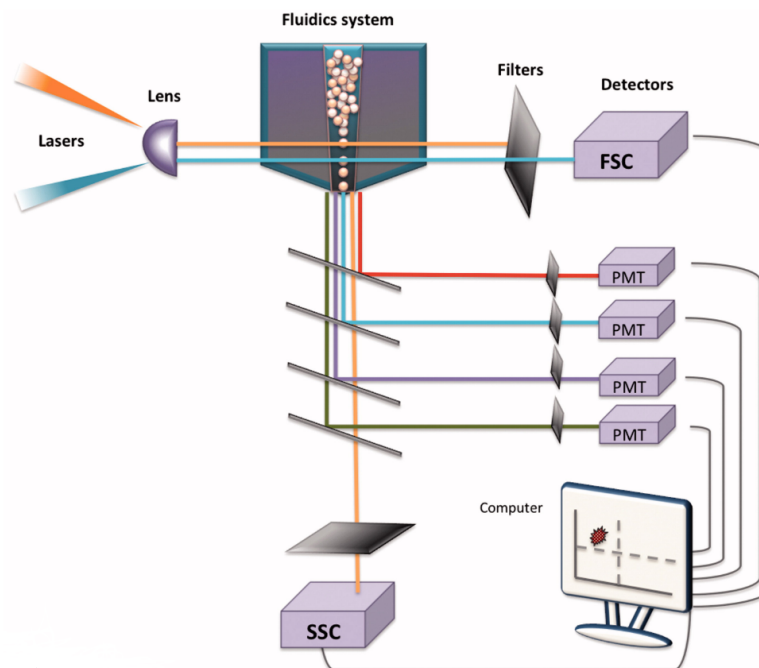


Figure 3. Flow cytometer. The cells are transported one-by-one through a fluidics system and hit by lasers. The FSC, SSC and fluorescence emission are detected by photodiodes or photomultiplier tubes (PMTs). The signals are converted into digital data that can be viewed as plots or graphs on a computer. (Adapted from [24])

4.4 Flowty Analysis

Flowty is an unpublished bioinformatic analytical application that has been used to perform subpopulation analysis and drug response data, using algorithms such as *FlowSOM* [10]. This section describes how to use Flowty and which analyses can be performed, whereas the Results & Discussion describes how it was used specifically to address the research questions.

The Flowty application can be opened in a browser after installing and running it in R. The first user interface presented is shown in Figure 4. Here the drug screen plate is processed by uploading an annotation file containing the compound and concentration information about each well along with the path to the FCS-files with the flow cytometry results. The control compound and what compounds to exclude in the analysis are also specified here. The biomarkers that are measured in the drug screen are automatically loaded into the `active channels`. The default plate is a 384-well plate, but the size of the plate can be changed. The `minimum events` are the lowest number of cells that should be detected in each well to include it in the analysis. The `sampling rate` is the proportion of each well that is randomly sampled when calculating global statistical summaries and channel correlations. `Quality control` and `signal drift correction` is performed by default, but can be turned off. Lastly, an absolute path to an output folder where the information of the analysis will be returned is entered before the screen can be processed.

Once the processing is finished, it is saved as an RData file and can be opened again in Flowty without having to run the plate again.

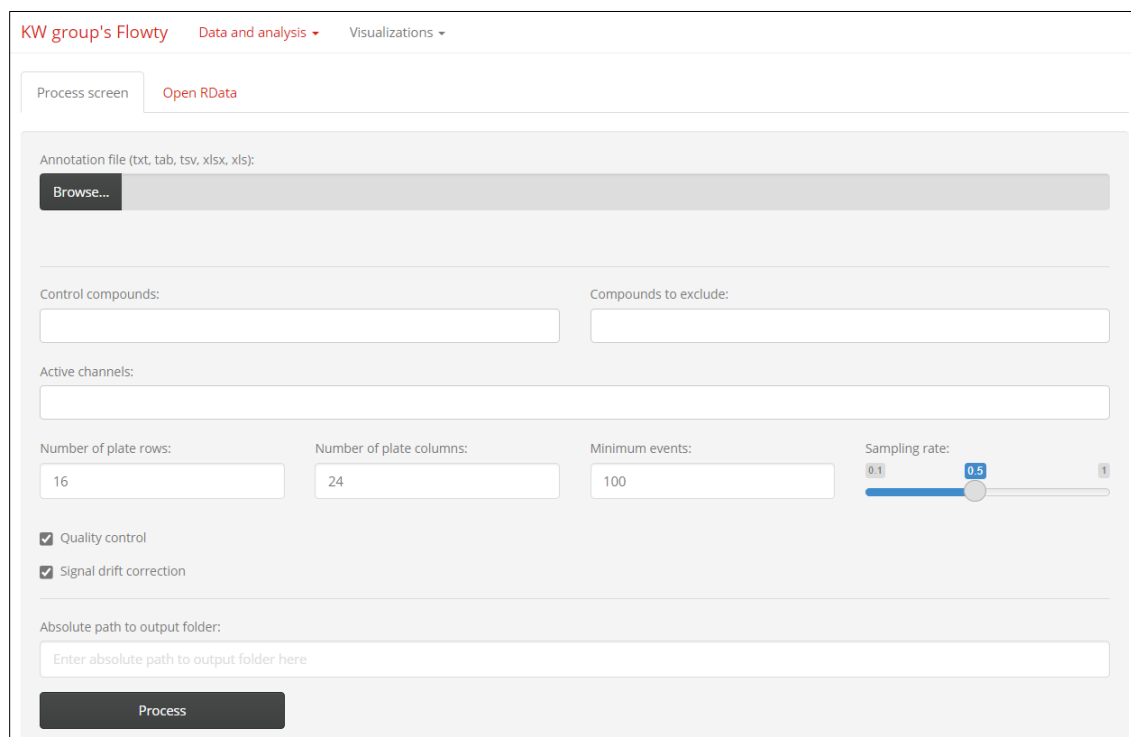


Figure 4. Flowty's "Data and analysis - Process screen" user interface.

When processing the data screen with quality control and signal drift correction, the fluorescent intensities are first compensated, filtered and then corrected to give more reliable results. In Flowty these adjustments can be viewed in a channel line plot (Figure 5). Channels which want to be viewed can be selected.

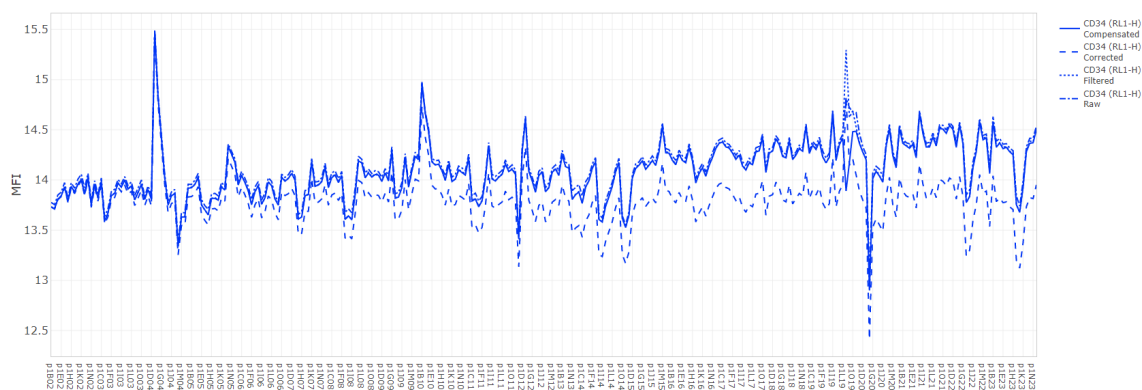


Figure 5. Channel line plot illustrating the raw, compensated, filtered and corrected mean fluorescence intensity (MFI) of CD34 expression across one plate in Flowty.

After the screen has been processed, clustering using the FlowSOM algorithm and differential abundance (DA) analysis can be performed (Figure 6).

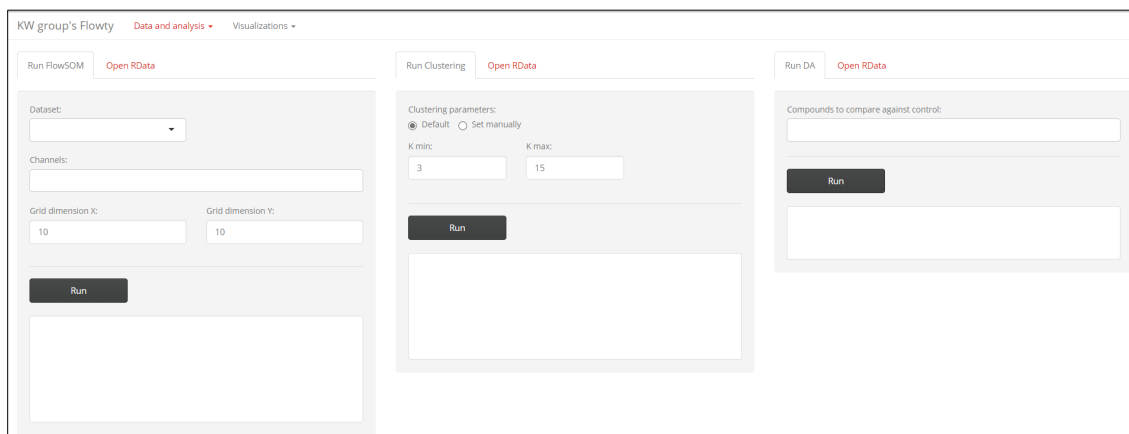
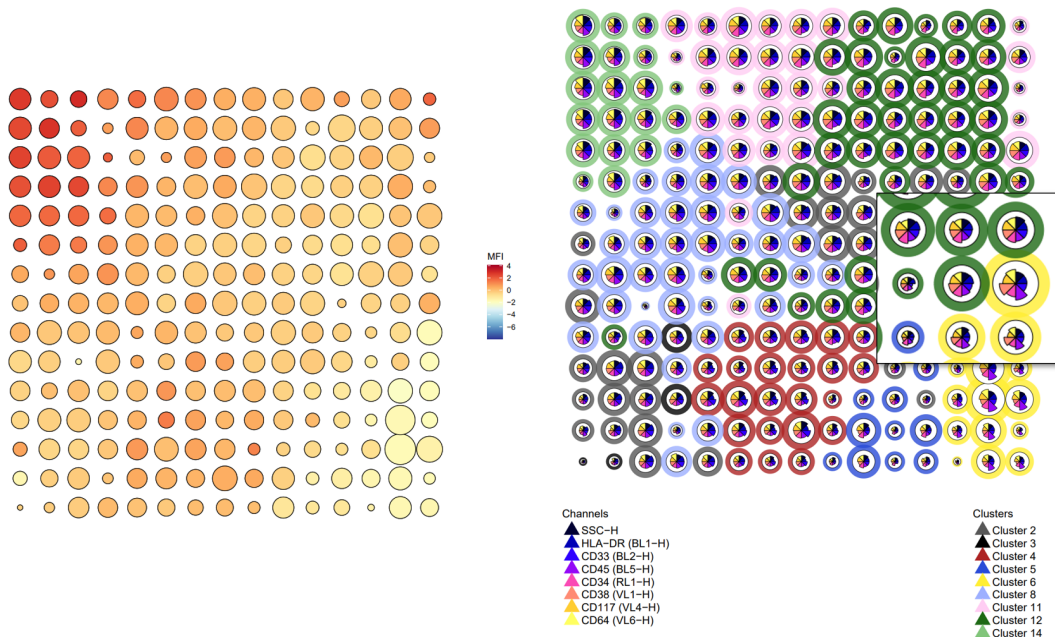


Figure 6. Flowty’s ”Data and analysis - Workflow” user interface.

The **dataset** and **channels** for the FlowSOM analysis are loaded by default after the screen has been processed. The dataset specifies whether to use the raw, compensated, filtered or corrected data, and is by default set to be the corrected. The channels, i.e., biomarkers, by which the cells are clustered can be adjusted. Simply explained, the FlowSOM algorithm initially places cells randomly into the grid of a self-organizing map (SOM) (Figure 7a). Each new cell is then compared, according to its phenotypic expression of the biomarkers, to the cells in the grid and placed with the most similar cell. The nodes are then compared to each other and rearranged according to similarity. More details about how the FlowSOM algorithm works can be found in the paper by Van Gassen, et al. [10].

After the cells have been placed in the SOM, an additional clustering of the nodes is performed to form the subpopulations (Figure 7b). This is done in the **clustering** window, see Figure 6, where you can select the minimum and maximum numbers of clusters (K_{\min} and K_{\max}) to be tested. By default, five different clustering algorithms are used, creating five times the number of K ($K_{\max} - K_{\min}$) cluster sets to be formed, one for each algorithm and cluster number. The significance of the cluster sets is then determined by the P-value created based on the null hypothesis, that is, the possibility that the clusters could be formed by chance. The significant threshold is set by default to a P-value of 5 %, but this can be adapted.



(a) The color of the nodes illustrates the intensity of the side scatter (SSC).

(b) the color of the SOM nodes indicates the subpopulation, with a star chart within illustrating the mean expression of each channel.

Figure 7. Self organizing maps (SOM) with a grid of 15x15.

4.5 Data Analysis

Flowty was used as the main analytical tool. The drug response data of the subpopulations obtained from Flowty was analyzed in Breeze. Breeze is a computational tool, introduced by Potdar et al. (2020), that performs qualitative drug response calculations on high-throughput drug screens. An Excel file is loaded, specifying the plate, well-id, subpopulation, compound, concentration and cell count. The application was set to perform inhibition readout with a four-parameter log-logistic model. Breeze then calculates the drug sensitivity score (DSS), which is used as a robust measurement of drug sensitivity [25]. The results from Breeze were extracted as matrices. All heatmaps were created in R using the R-package *ComplexHeatmap* [26]. All clustering analyses were performed using the complete linkage clustering method with Euclidean distance.

5 Result & Discussion

5.1 Which Are the Least Differentiated Cells, and Their Phenotypes, in Each AML Patient?

This research question aimed to establish an automated method for comparing AML patients. This could then be used for exploring whether similar types of AML have a similar drug response, and recognize potential drugs targeting the least differentiated cells, possibly leukemic stem cells. By using Flowty, analysis of the highly diverse cellular phenotypes within and between patients with AML could be studied in more depth than using traditional manual gating strategies.

5.1.1 Identifying and Characterizing Subpopulations

The first approach was to run all patient plates in Flowty individually. The FlowSOM grid dimensions were 15x15 and the number of clusters (K), i.e. subpopulations, were set to be between 3-15 for each run. The cluster sets used were the ones with the highest significance score, indicating clusters containing the most similar cells.

To compare the cellular subpopulations within and between the patient samples, the subpopulation heatmaps were extracted for each patient (Figure 8). The subpopulation heatmaps, for each patient, were then looked at individually to find the least differentiated subpopulation for each AML patient.

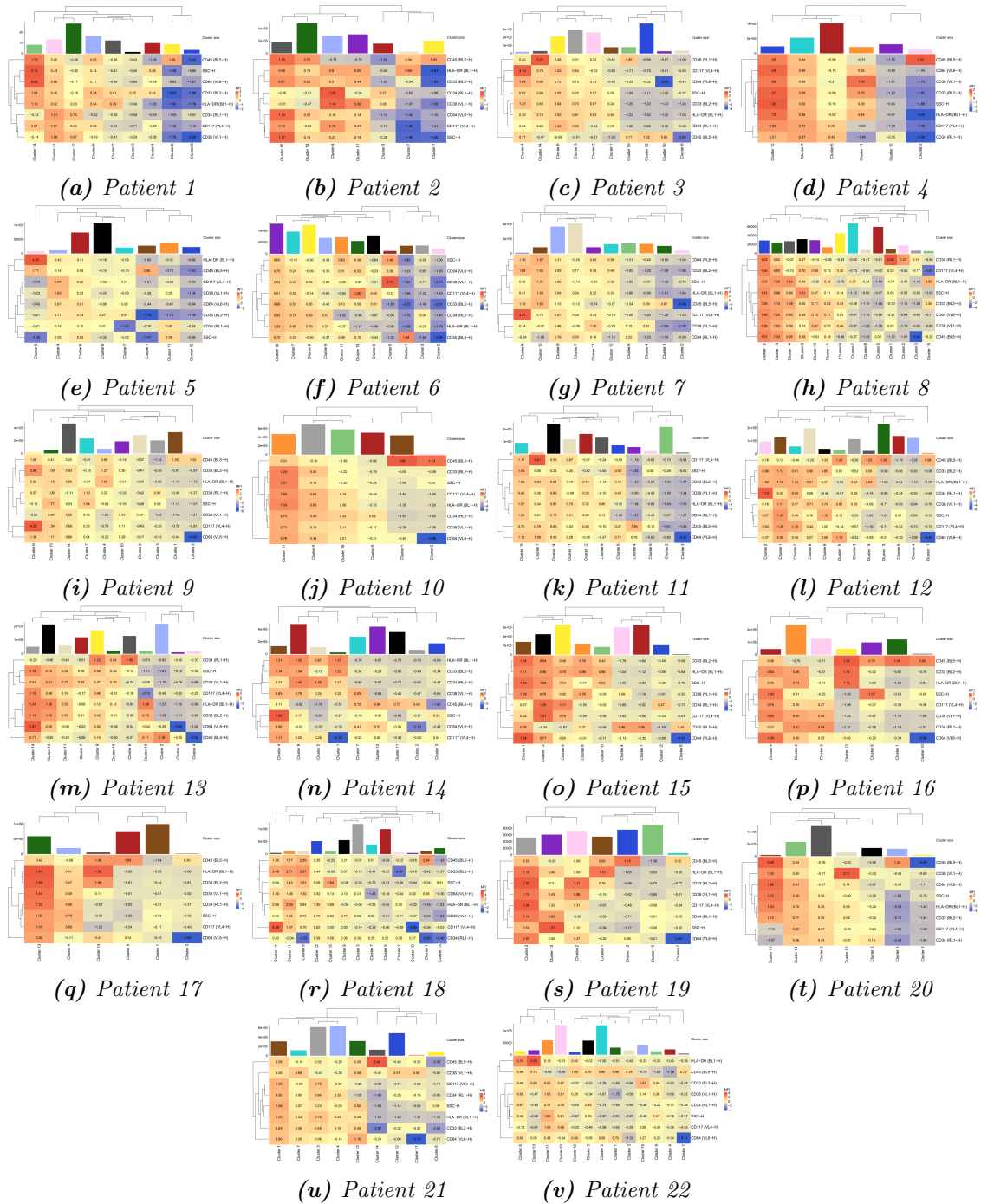
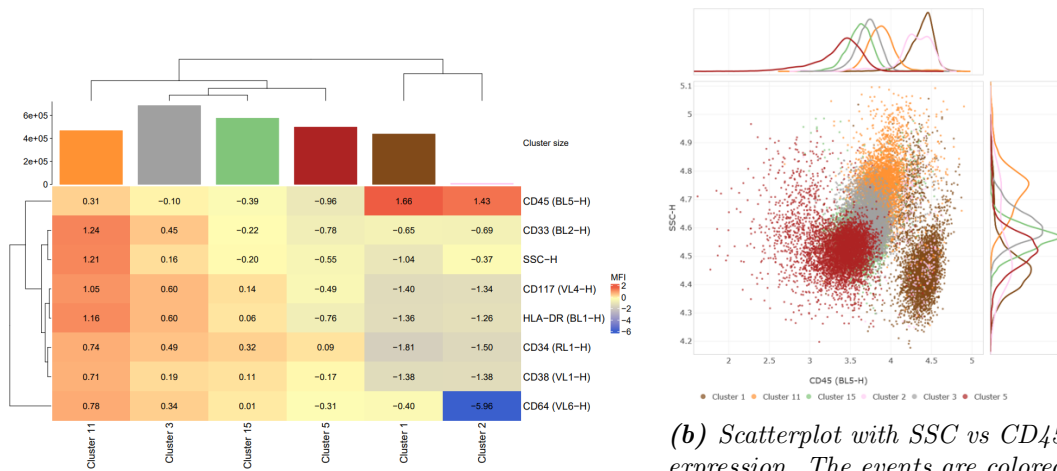


Figure 8. Subpopulation heatmaps for all patients, illustrating the cellular subpopulations (columns) and their phenotypic expression (rows). The bar plot illustrates the size of the subpopulation, measured in cell count. The dendrograms illustrate the hierarchical clustering of the subpopulations and biomarkers, according to the phenotypic expressions measured as mean fluorescent intensity (MFI).

In Figure 9, a representative patient (patient 10) is illustrated. Here, the subpopulation heatmap (Figure 9a) shows the six subpopulations of the patient derived cells. According to the phenotypic expression, the least differentiated subpopulation is number 5, which only express CD34. This subpopulation mimic the expression of early myeloid progenitors, as seen in the myelopoiesis in figure 1.

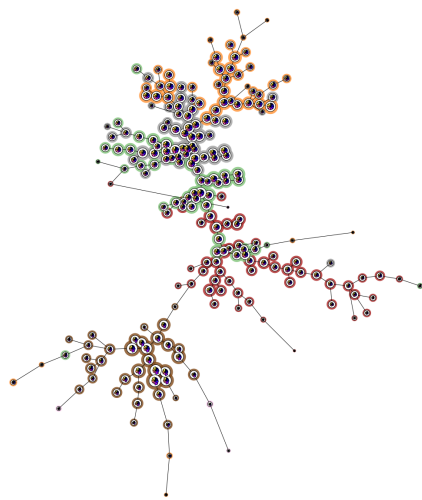
An alternative approach to compare the subpopulations in Flowty is by visualizing them in a scatterplot. In the scatterplot, biomarkers for comparison can be selected. In Figure 9b, the side scatter (SSC) is plotted against the CD45 expression. The least differentiated cells are expressed in the lower left corner, having low SSC and CD45 expression, which in this case is represented by subpopulation 5. During differentiation, the cells progressively express more CD45 and becomes more granular, which is represented by the SSC. This indicates that the order of differentiation after subpopulation 5 is 15, 3 and lastly 11. The lower right subpopulation 1 is the typical lymphocyte subpopulation, having high CD45 expression and a low SSC. Subpopulation 2 is less than 1% of the cells and has an extremely low CD64 expression. This is most probably an outlier that is not relevant to look at due to the size of the cluster.

The minimal spanning tree (MST) generated by Flowty (Figure 9c) arranges the SOM nodes according to their phenotypic expression in relation to each other. The MST shows the least differentiated subpopulation nodes in the middle. Lymphocytes are represented on one branch, whereas the three branches correspond to other myeloid subpopulations differentiating/growing out in another direction. The interpreted differentiation hierarchy and the assumptions made about the lymphocyte and outlier subpopulations are shown in Figure 9d.

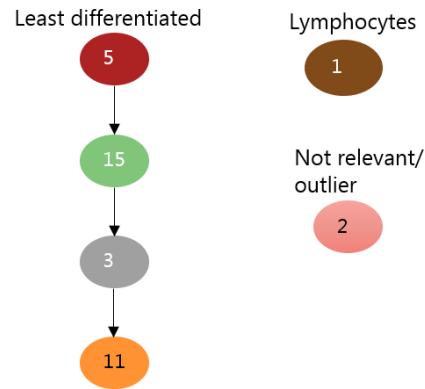


(a) Subpopulation heatmap. Each cluster represents a subpopulation.

(b) Scatterplot with SSC vs CD45 expression. The events are colored according to their distributed subpopulation.



(c) Minimal spanning tree (MST) of the SOM nodes. The color of the nodes represents the subpopulations.



(d) The interpreted differentiation hierarchy of the subpopulations, as well as lymphocytic and an outlier subpopulation.

Figure 9. Subpopulation analysis of patient 10.

Investigating the other patients using the same approach as described above was challenging. The subpopulations' phenotypic expression of the biomarkers does not always correspond to a specific cell type in the myelopoiesis (Figure 1), and for patients not having a clear CD34+/CD38- population, it was therefore difficult to determine the least differentiated subpopulation. The MFI values are also normalized for each patient when run through Flowty, making them non-comparable between patients. After attempts to build differentiation patterns for the patients, as done for patient 10, the comparison of patients was done based on comparable subpopulations, generated together for all patients in Flowty, instead.

5.2 Do Similar Differentiating AML Patients Have Similar Drug Response?

5.2.1 Comparing Patients Based on Subpopulation Composition

In contrast to running the patient plates one-by-one in Flowty, running all plates together would create comparable subpopulations since the phenotypic expressions are normalized across all patient cells. However, the Flowty analysis generates a lot of memory, not being compatible with some of the R-packages used in Flowty, or the RAM memory of the computer. This limitation prevented Flowty analysis of all 22 patient plates together. Therefore, to reduce the memory of the analysis, only the 16 untreated control wells of each patient were run together in Flowty. In order to create significant cluster sets, generating subpopulations for all 22 patients, the *FlowSOM* grid was increased to 35x35 and *K* was set to be between 30-40, after trying out different options. The subpopulations with the highest significance are shown in Figure 10.

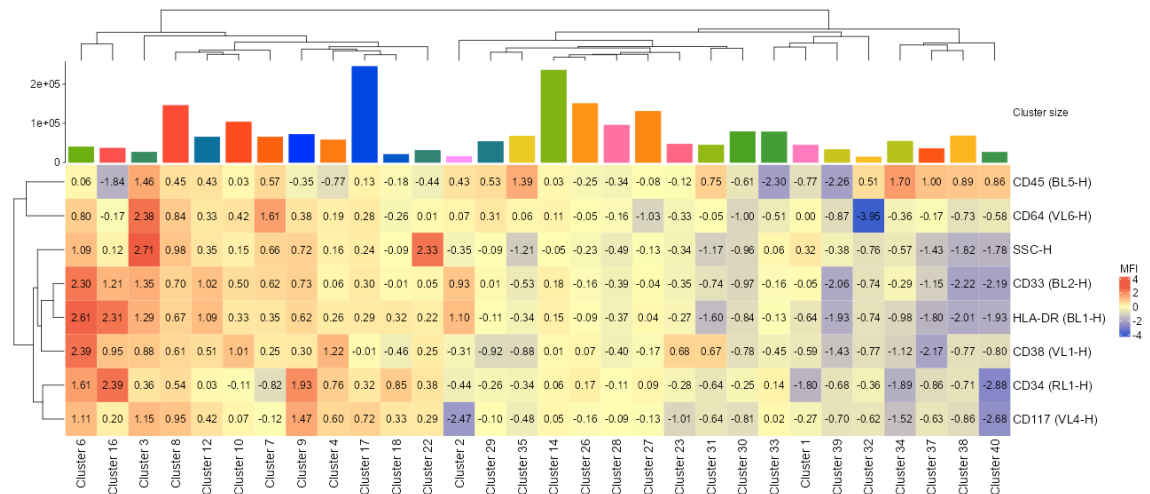


Figure 10. Subpopulation heatmap showing the 30 subpopulations generated when running all 22 patient control wells together in Flowty.

By comparing the subpopulation composition of each control well, it may be possible to identify patients with similar phenotypic differentiation patterns. The subpopulation bar plot, in Figure 11, illustrates the percentage of the subpopulations in each patient's 16 control wells. It is possible to get a visual overview of the phenotypic differences between patients.

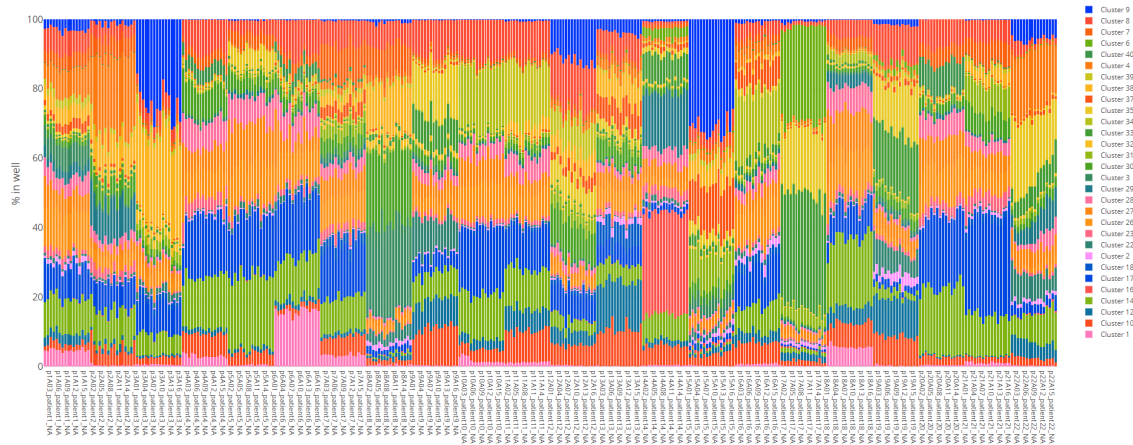


Figure 11. Subpopulation bar plot showing the percentage of each subpopulation in the 16 control wells of the 22 patients. The colors indicate the 30 different subpopulations shown in the subpopulation heatmap. The patients are shown in increasing order.

However, to determine which AML patients shows similar phenotypic differentiation patterns, a quantitative comparison of the subpopulation composition data is needed. Therefore, a heatmap in which the wells are clustered according to their subpopulation composition was created (Figure 12). The subpopulations that looked like lymphocytes (subpopulation 32, 34, 35, 37, 38 and 40 in the subpopulation heatmap) were removed since the main interest lies in investigating the myeloid cell populations, which are the potential leukemic cells.

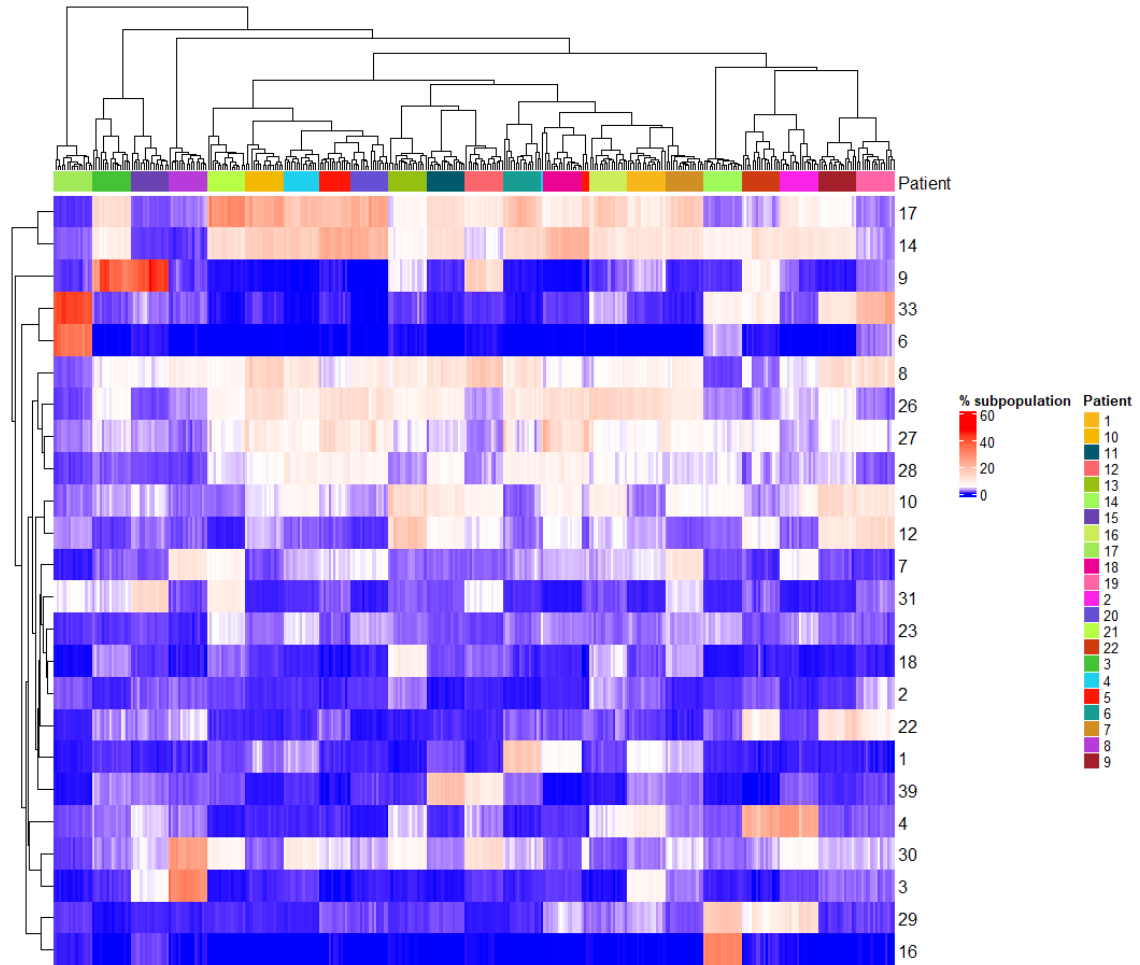


Figure 12. Heatmap showing the 16 untreated patient control wells (columns) and their subpopulation percentage for each subpopulation (rows). The dendrogram on top shows the hierarchical clustering of the wells. The dendrogram connects the wells based on similarity, where more similar wells are connected further down. The subpopulation numbers corresponds to the numbers in the subpopulations heatmap (Figure 10).

The dendrogram on top of the heatmap illustrates the clustering of the wells based on their subpopulation composition similarity. The control wells are clearly clustered according to patient, indicating patient control well similarity, which is positive for further analysis. The dendrogram also shows similarities between patients, with some patients being more similar than others. These results can be used in further analysis to investigate whether patients with similar subpopulations have similar drug response.

5.2.2 Analyzing the Relationship Between Subpopulation Composition and Drug Response across Patients

The subpopulation composition of all patients was compared to the drug response of all cells, excluding the lymphocytes, to see whether similar differentiating AMLs exhibit a similar drug response. The drug sensitivity score (DSS) was calculated to determine the total drug response for all cells, for each drug and patient. The subpopulation composition was determined by calculating the average subpopulation percentages in the control wells.

The FAB class, gender, age, cell count, mutations and karyotype of the patients were also included in the analysis to see whether they had any obvious correlation to the drug response. All these data were combined in a heatmap (Figure 13).

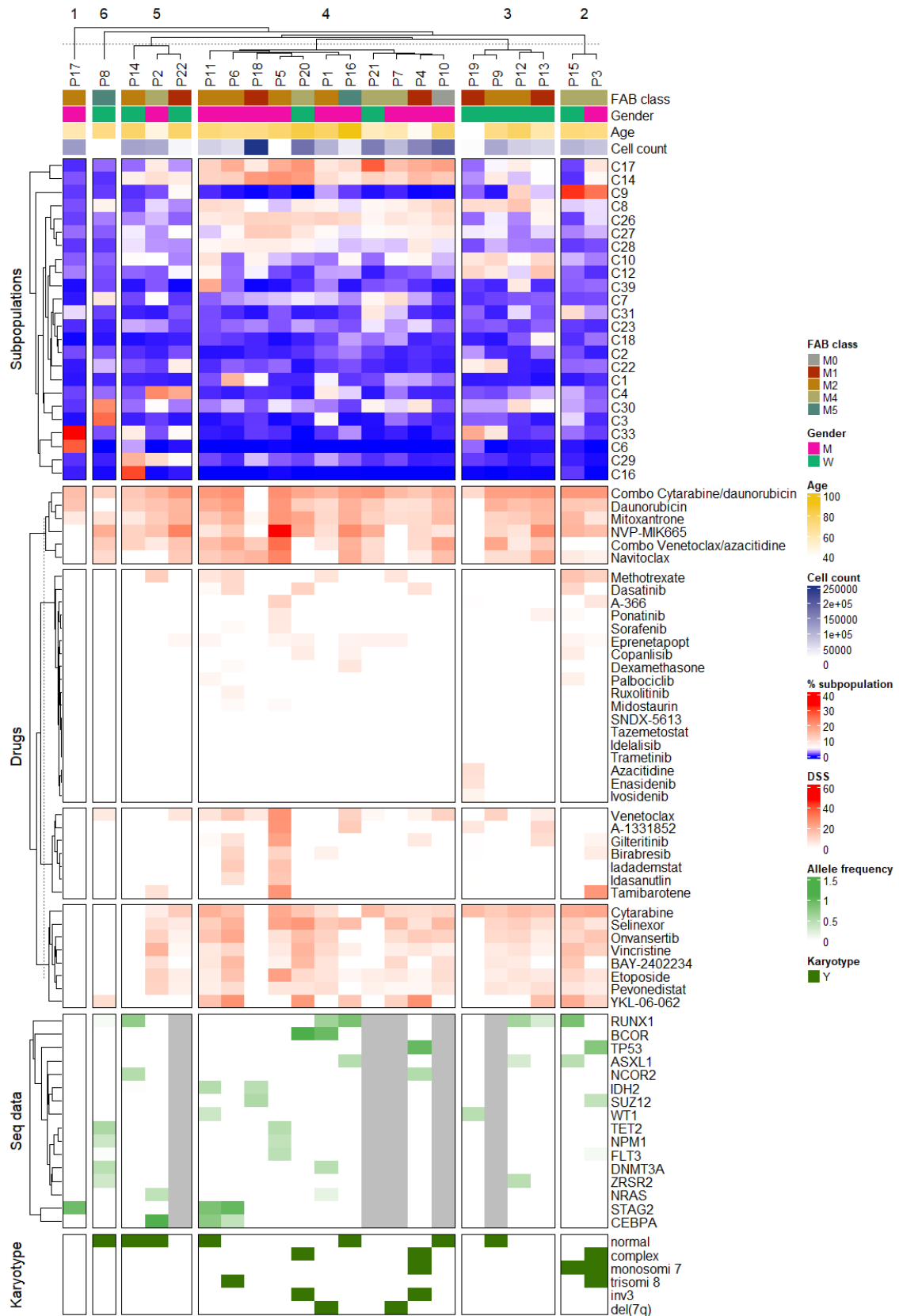


Figure 13. Heatmap showing the patients (columns) and their subpopulation composition, drug sensitivity scores (DSS), mutations from sequencing (seq) data existing in two or more patients, and karyotype (rows). The FAB class, gender, age and total cell count of all subpopulations, except the lymphocytes, is annotated for each patient. The dendrogram on top shows the hierarchical clustering of the patients based on their subpopulation composition and divides the patient into six groups.

Patients with similar subpopulations, or phenotypic differentiation, do not show any obvious correlations in their overall drug response. No clear correlations in the mutational and karyotypic expressions to the drug response can be observed either. There are variations between patients showing very similar subpopulation compositions, as for example patient 5 and 18, while other similar patients, such as 15 and 3, show more similar drug response. This highlights the complexity of the disease. Individual drug responses across patients could be compared between similar differentiating AML and/or genetic data, to investigate further on how specific drugs target different AML. However, this was not in the scope of this project. To answer the research question on whether similar differentiating AML have a similar drug response, a larger patient cohort would be required to generate more significant results, where the responses could be statistically compared between different groups of similar AML. In addition, the drug response of patients should preferably also be analyzed on different cell subpopulations and not solely on the overall drug response of the bulk cells.

5.3 Do Similar Subpopulations, Between Different AML Patients, Have Similar Drug Response?

AML is a very heterogeneous disease, and it is crucial that the optimal treatment for each patient is found. Therefore, predictive characteristics of patients need to be established. If AML precision medicine should be guided by phenotypic characterization of hierarchical subpopulations, it is essential to examine whether these subpopulations exhibit similar drug responses across different patients.

5.3.1 Drug Response Analysis of Subpopulations across Multiple Patients

To compare the subpopulation drug response between AML patients, the whole plates with all the drug wells need to be included in the Flowty analysis. Due to limitations in running multiple plates together in Flowty, four groups, a total of nine patients, were selected for this analysis. The patients were chosen based on the hierarchical clustering of the patients' subpopulation composition seen in figure 12. Patients with similar subpopulation expressions were selected, and groups were formed based on their dissimilarity between each other. These groups are (A) patient 3 and 15, (B) patient 4, 5 and 20, (C) patient 2 and 22 and (D) patient 9 and 19.

The drug screening plates from the nine chosen patients were run together in Flowty. The clustering analysis was performed several times, testing different numbers of clusters (K). High significance was shown for cluster sets consisting of 13 and 21 subpopulations. To ensure larger subpopulations for further analysis, the cluster set of 13 subpopulations was selected. These subpopulations are therefore larger, consisting of a higher variability of cells. Consequently, they have a higher representation across patients, allowing for meaningful comparisons between patients. The 13 subpopulations that were generated for the nine patients are shown in Figure 14.

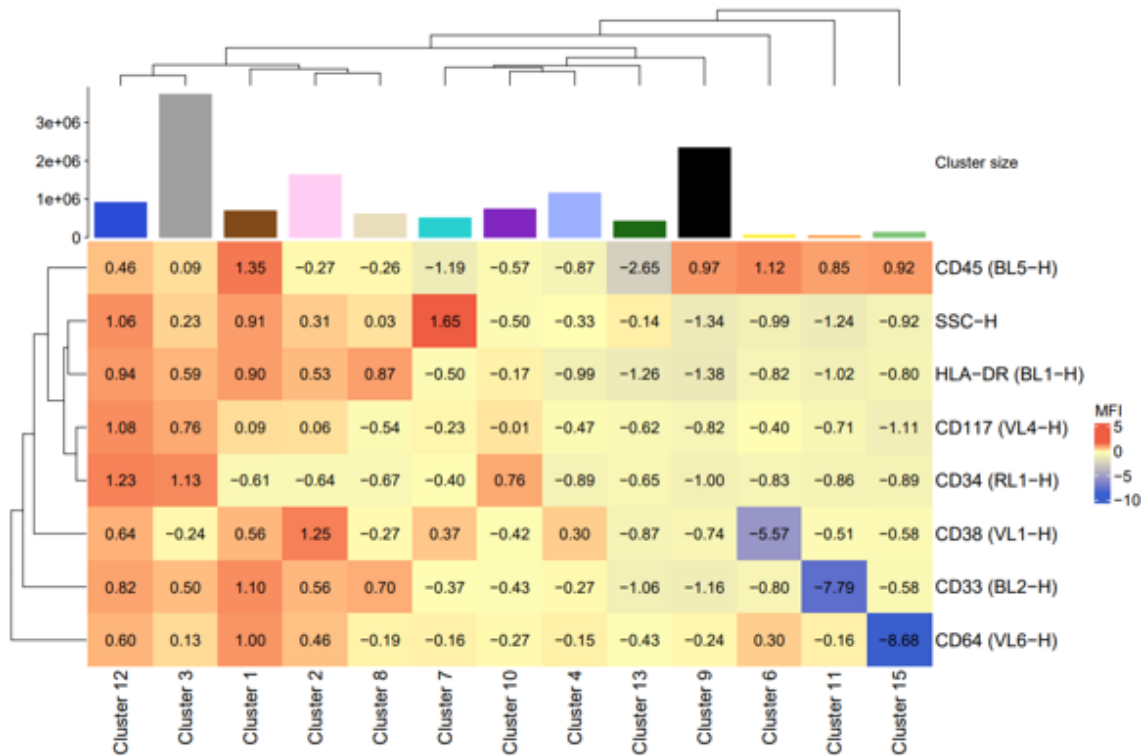


Figure 14. Subpopulation heatmap showing the phenotypic expression of the 13 subpopulations obtained running patients 2, 3, 4, 5, 9, 15, 19, 20 and 22 together in Flowty.

The drug response data for each subpopulation and patient, represented as cell count, was extracted from Flowty. To solely focus on the potential leukemic cells and their drug response, the lymphocytes (subpopulation 9, 6, 11, and 15) were removed from further analysis. The subpopulation composition of the nine patients is shown in Figure 15.

Prior to investigating the subpopulation drug response, the data was filtered to avoid misleading results. The standard deviation of the cell count of the subpopulations in the patient control wells was calculated. Subpopulations exceeding a standard deviation of 22% were excluded from further drug response analysis. Only three subpopulations (2, 3 and 4) had a lower standard deviation in two or more of the patients. These subpopulations and patients are marked with asterisks in Figure 15.

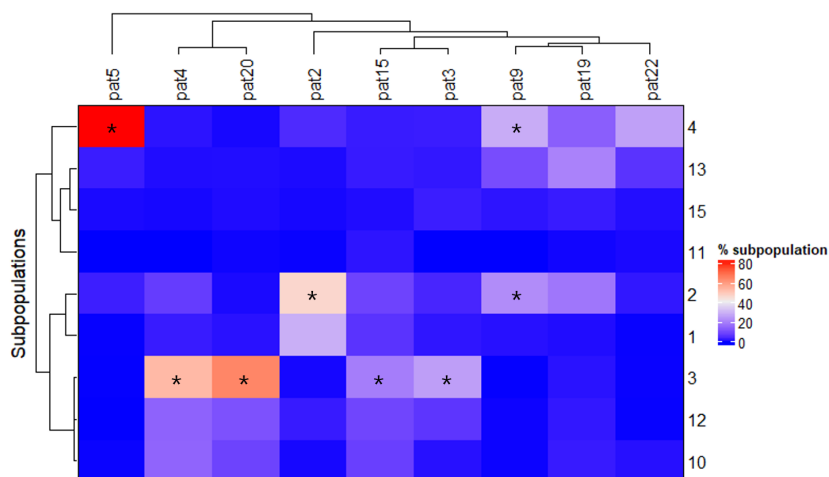


Figure 15. Heatmap showing the subpopulation composition of patient 2, 3, 4, 5, 9, 15, 19, 20 and 22. The subpopulations correspond to the subpopulations in Figure 14. The asterisks mark the subpopulations of patients with substantial amount of cells to be used as a negative control for the drug response comparisons, having less than 22% standard deviation in the control wells of at least two patients.

The DSS derived from the drug response analysis in Breeze is illustrated as a heatmap in Figure 16. The subpopulations are clustered together according to the dendrogram, independent of the patient, indicating that similar subpopulations have similar drug response. Nevertheless, there are still some variations between the subpopulations that cluster together, indicating patient variability. However, to obtain significant results regarding subpopulation drug response across patients and to compare patient variability, it would be necessary to have additional subpopulations and patients to compare.

In order to obtain additional comparable subpopulations, the cell count in each well would need to be increased. This should contribute to lower standard deviation in the control wells, making the drug response calculations more robust. This analysis could therefore not focus on patient similarity, but rather on subpopulation similarity independent of patient.

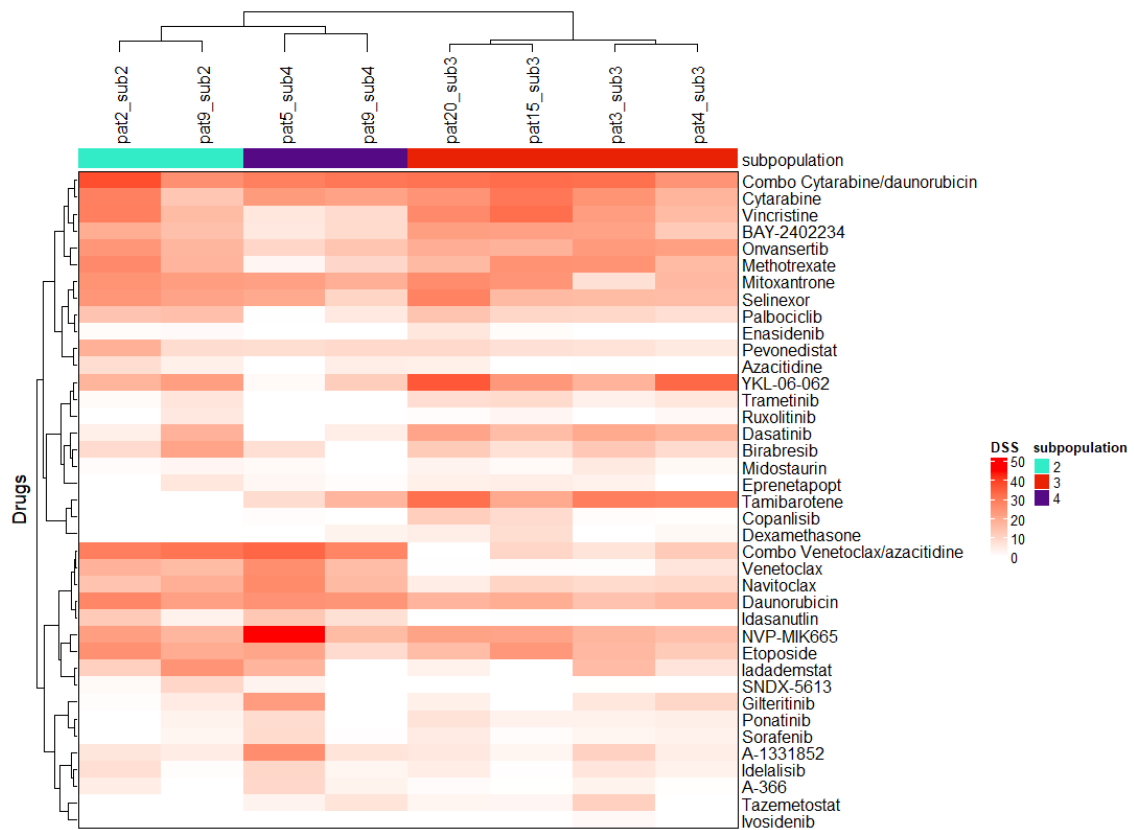


Figure 16. Heatmap showing the DSS of subpopulation 2, 3 and 4.

By looking at the drug responses one drug at a time, some drugs seem to have an effect on all three subpopulations, indicating no subpopulation specificity, while others seem to work only for one or two of the subpopulations. For example, the combination therapy with cytarabine and daunorubicin, at the top of the heatmap, seem to be effective on all three subpopulations, whereas the other combination therapy with venetoclax and azacitidine seems to be effective only on subpopulation 2 and 4, not on 3. The drug response curves of the combo venetoclax/azacitidine, obtained from Breeze, is shown in Figure 17, together with the DSS bar plots.

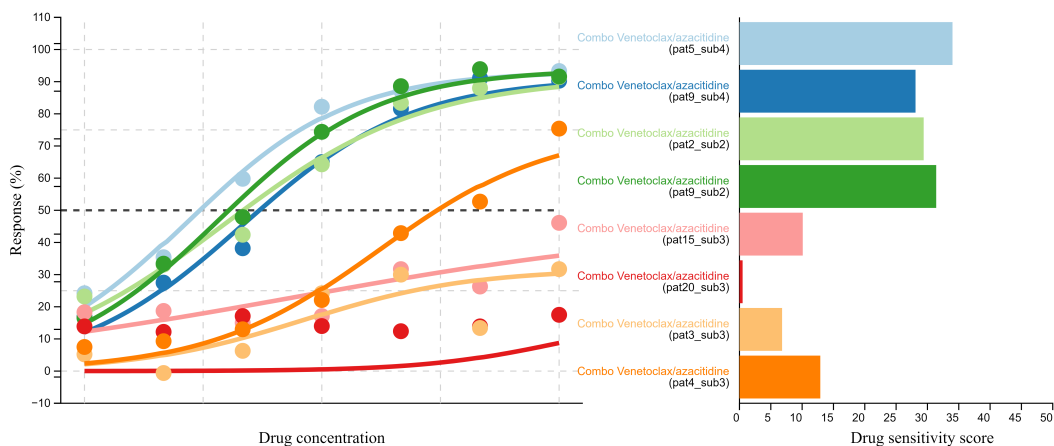


Figure 17. Drug response curves and DSS bar plots for subpopulation 2 (green colors), 3 (red colors) and 4 (blue colors), taken from seven different patients, for Combo Venetoclax/azacitidine treatment.

5.3.2 Drug Response Analysis of Subpopulations from Individual Flowty Runs

The same approach as described above should be performed on more subpopulations and patients to obtain statistically significant results to fully answer the research question. This would also enable further analysis of which subpopulations respond to which drugs. However, due to the limitations already mentioned, the number of plates being run together in Flowty was restricted. Therefore, the subpopulations generated from the individual Flowty runs (Figure 8) were chosen for drug response comparison.

Although the MFI values of the subpopulations in the individual Flowty patient analysis were normalized for each plate, it is uncertain whether the observed variations in MFI are specifically influenced by the patient. To investigate this, a factor analysis was performed. Principal component analysis (PCA) on the subpopulations based on their MFI (Figure 18) was executed. A regression analysis of each principal component against the patient covariate was performed, showing no sign of patient-dependent variations. This can also be seen by looking at the PCA plot.

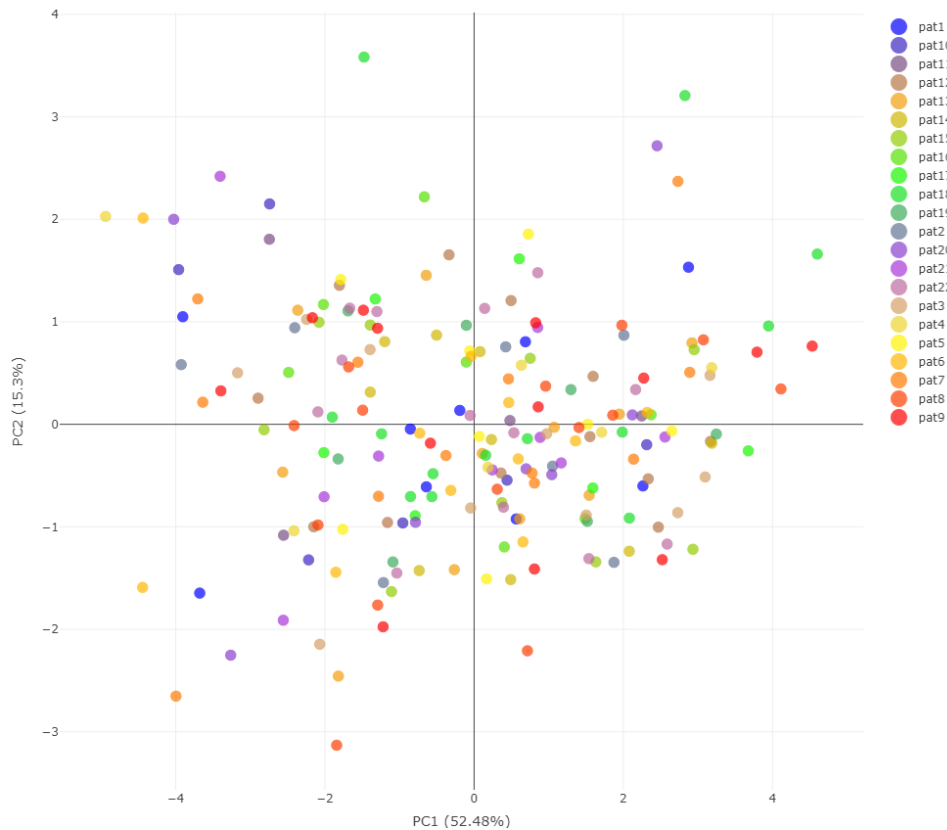


Figure 18. PCA plot showing how the patient subpopulations are distributed based on their MFI values.

Drug response analysis was therefore performed for each subpopulation, generated from the individual Flowty runs. Before the analysis, subpopulations showing a standard deviation higher than 22% in the control wells were filtered out. The biomarker expression (measured as MFI) and the drug response (measured as DSS) are illustrated for each of these subpopulations in Figure 19.

The heatmap illustrates 10 groups of subpopulations, based on the hierarchical clustering of the MFI. Group 2, 3 and 4 consists of lymphocytes, whereas group 1 are probably subpopulations of dead cells that were not removed during the manual gating. These groups show significantly less drug response compared to the other subpopulations, which is expected. The other subpopulations exhibit a varying phenotypic expression. Group 6 appears to consist of less differentiated cells, having low expression of biomarkers but showing a higher expression of CD34. Group 10 seems to consist of more differentiated cells, with high granularity (SSC). The other groups, 5, 8, 7 and 9 consist of various AML blasts that will not be further characterized.

The drug response within these AML blast subgroups are varying between subpopulations. However, the overall drug response pattern appears to be similar, where some drugs have a greater impact than others. The observed variability could be patient-dependent, however, this is difficult to outline in this heatmap. Therefore, the heatmap was rearranged ordering the subpopulations based on patient, instead of marker expression (Figure 20).

The drug response of subpopulations within each patient exhibit more similarity than the subpopulations compared across patients, indicating that cells within one patient are more similar in differentiation. However, the drug response within each patient also varies across subpopulations, indicating that subpopulations with different phenotypic expression show different responses within patients as well.

The heterogeneity between (Figure 19) and within (Figure 20) patients become evident when comparing the two heatmaps. This demonstrates the complexity of the disease. The only clear correlation that can be seen, is the difference between the lymphocytes and the rest of the AML blasts (Figure 19). Statistical analysis of the DSS between the subpopulation, such as ANOVA, could reveal if there are subpopulation dependencies in the drugs, but were limited due to time constraints.

These subpopulations drug response heatmaps have only clustered subpopulations and patients independently of one and another. If subpopulation and patient similarities were combined before looking at the drug responses, it would be possible to investigate whether similar subpopulations, in similar differentiating AML, have comparable drug responses. This analysis was also limited due to time constrains.

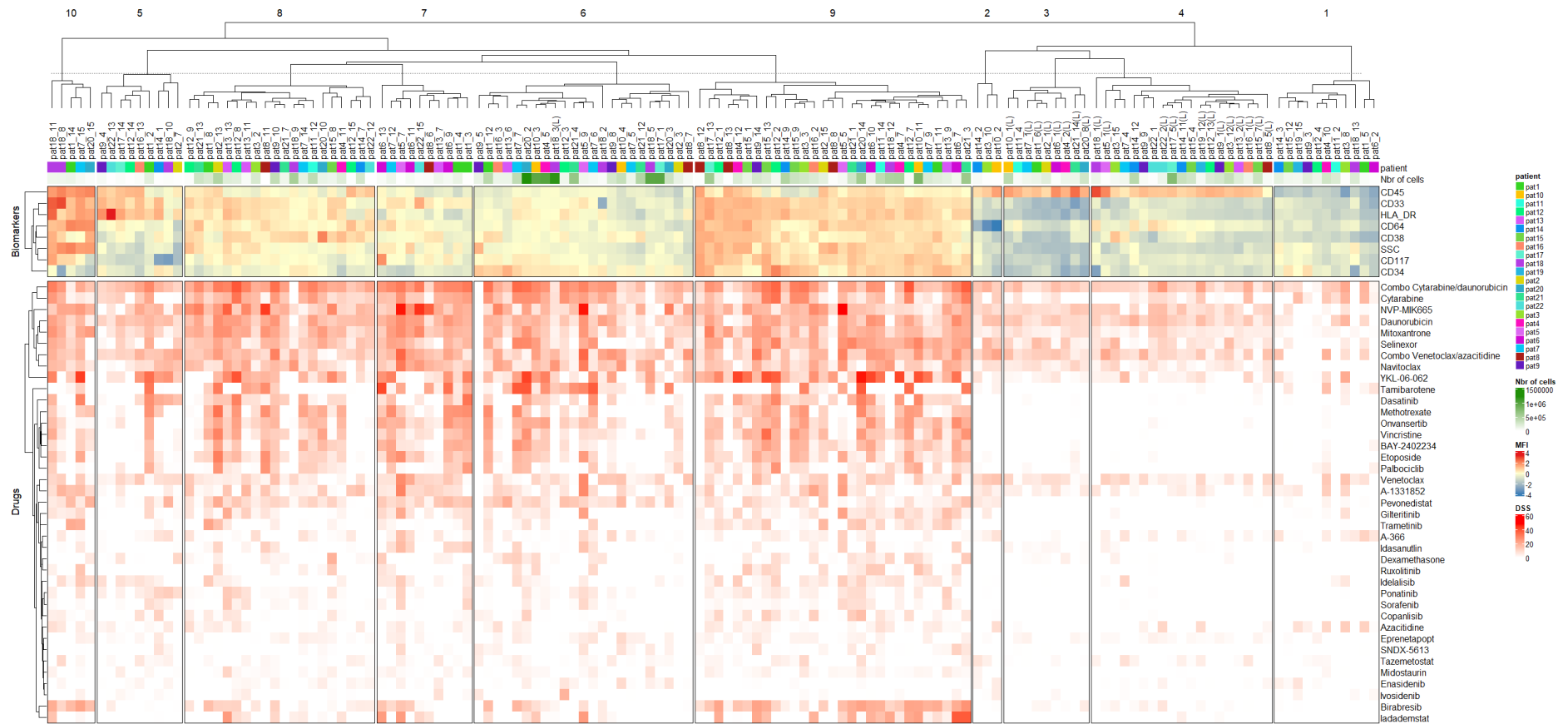


Figure 19. Heatmap showing the subpopulations from each individual Flowcy run and their phenotypic expression and DSS for the different drugs. The patient and the cell count are annotated on top. The dendrogram shows the hierarchical clustering of the subpopulations based on their phenotypic expression of the biomarkers. The subpopulations are divided into 10 groups.

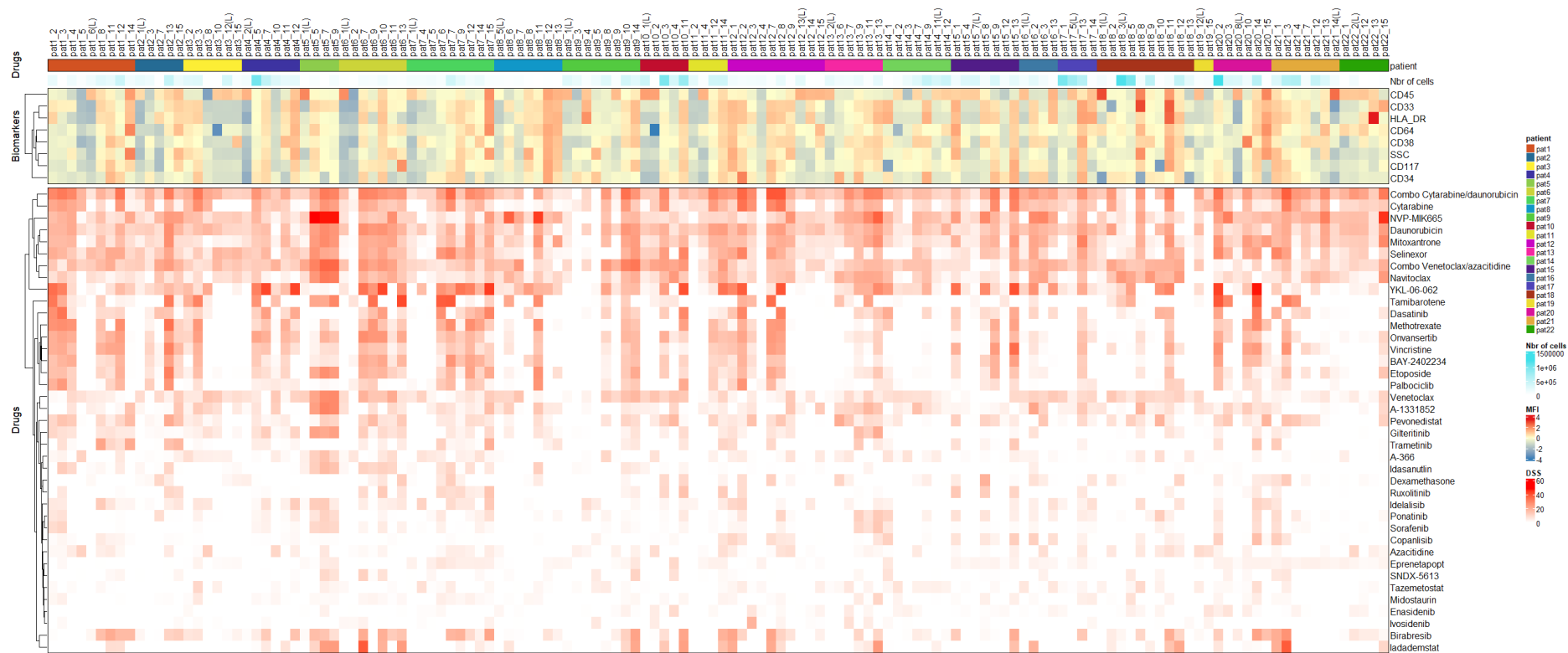


Figure 20. Heatmap showing the subpopulations from each individual Flowty run and their phenotypic expression and DSS for the different drugs. The patient and the cell count are annotated on top, and the subpopulations are ordered by patient ID.

6 Future Aspects

To obtain more accurate clustering of patients according to their phenotypic expressions, the subpopulations that are compared between patients should first be compared and clustered to each other based on their phenotypic expression. Thereby, patients expressing distinct subpopulations yet similar, can be detected and clustered more closely together. Additionally, a larger patient sample size would improve the characterization, with more and larger patient subgroups to be analyzed.

To see whether similar subpopulations show similar drug response results within similar patients, the subpopulation drug response within and between patient subgroups should be analyzed. This would generate a three-dimensional matrix of patient subgroups, subpopulations and drug response data. A high-throughput approach for statistical analysis of such data would also need to be established.

When analyzing the drug response of subpopulations, it is also interesting to see whether the cellular subpopulation increases in number, indicating differentiation towards that subpopulation caused by a drug. To do this, a high-throughput analysis of investigating both inhibition and proliferation drug responses has yet to be found.

7 Conclusion

Flowty can be used to automatically visualize subpopulations from flow cytometry data. It was difficult to create an automated way of determining the hierarchical differentiation of each patient, due to the complexity of the phenotypic expressions shown for each subpopulation. Instead, patients were compared by analyzing the composition of subpopulations generated together for all patients, indicating patients with similar differentiation. However, to improve this, a prior clustering of the subpopulations based on phenotypic expression would enhance the analysis by adding an extra comparative dimension.

Due to high heterogeneity between patients, most subpopulations were only highly expressed in few of the 22 patients, and the rest of the subpopulations were only present in a very low number. Therefore, there were few subpopulations that could be properly compared across patients based on their drug response. Larger patient cohorts and a higher cell number per well would improve the analysis. Comparing the subpopulations generated in the individual Flowty runs, variations between subpopulations were shown both between and within patients, indicating the complexity of this heterogeneous disease. To evaluate whether similar subpopulations have similar drug response, the conclusion was that patients with phenotypic similarities should be grouped together before comparing the drug response. It would then be possible to investigate whether similar subpopulations show similar drug response in similar differentiating AML, which would possibly generate more apparent results.

Even though this research project did not generate any statistically significant results, it introduced potential methodologies that can be used in further research. This includes how

Flowty can be used in order to do cellular subpopulation analysis of patient flow cytometry drug screens, and how AML patients can be compared based on their subpopulations, and subpopulation drug response. To improve clinical outcomes for patients with AML, the identification of predictive biomarkers to guide precision medicine is crucial and further research within phenotypic expressions and drug responses between patients still holds this promise.

References

- [1] Fatemeh Pourrajab, Mohamad Reza Zare-Khormizi, Azam Sadat Hashemi, and Seyedhossein Hekmatimoghaddam. Genetic characterization and risk stratification of acute myeloid leukemia. *Cancer management and research*, 12:2231, 2020.
- [2] National Cancer Institute. Acute myeloid leukemia - cancer stat facts. <https://seer.cancer.gov/statfacts/html/amy1.html>, 2022.
- [3] Shyam A Patel and Jonathan M Gerber. A user’s guide to novel therapies for acute myeloid leukemia. *Clinical Lymphoma Myeloma and Leukemia*, 20(5):277–288, 2020.
- [4] Kari Hemminki, Janne Hemminki, Asta Försti, and Amit Sud. Survival in hematological malignancies in the nordic countries through a half century with correlation to treatment. *Leukemia*, 37(4):854–863, 2023.
- [5] Sabine Kayser and Mark J Levis. Updates on targeted therapies for acute myeloid leukaemia. *British journal of haematology*, 196(2):316–328, 2022.
- [6] Brian S White, Suleiman A Khan, Mike J Mason, Muhammad Ammad-Ud-Din, Swapnil Potdar, Disha Malani, Heikki Kuusanmäki, Brian J Druker, Caroline Heckman, Olli Kallioniemi, et al. Bayesian multi-source regression and monocyte-associated gene expression predict bcl-2 inhibitor resistance in acute myeloid leukemia. *NPJ precision oncology*, 5(1):1–11, 2021.
- [7] Hélène Pasquer, Maëlys Tostain, Nina Kaci, Blandine Roux, and Lina Benajiba. Descriptive and functional genomics in acute myeloid leukemia (aml): paving the road for a cure. *Cancers*, 13(4):748, 2021.
- [8] Zahid Kaleem, Eric Crawford, M Hanif Pathan, Leah Jasper, Michael A Covinsky, Lawrence R Johnson, and Glenda White. Flow cytometric analysis of acute leukemias: diagnostic utility and critical analysis of data. *Archives of pathology & laboratory medicine*, 127(1):42–48, 2003.
- [9] Lukas M Weber, Malgorzata Nowicka, Charlotte Sonesson, and Mark D Robinson. diffcyt: Differential discovery in high-dimensional cytometry via high-resolution clustering. *Communications biology*, 2(1):183, 2019.
- [10] Sofie Van Gassen, Britt Callebaut, Mary J Van Helden, Bart N Lambrecht, Piet Demeester, Tom Dhaene, and Yvan Saeys. Flowsom: Using self-organizing maps for visualization and interpretation of cytometry data. *Cytometry Part A*, 87(7):636–645, 2015.
- [11] Kipp Weiskopf, Peter J Schnorr, Wendy W Pang, Mark P Chao, Akanksha Chhabra, Jun Seitani, Mingye Feng, and Irving L Weissman. Myeloid cell origins, differentiation, and clinical implications. *Myeloid Cells in Health and Disease: A Synthesis*, pages 857–875, 2017.

- [12] Nicolas Goardon, Emanuele Marchi, Ann Atzberger, Lynn Quek, Anna Schuh, Shamit Soneji, Petter Woll, Adam Mead, Kate A Alford, Raj Rout, et al. Coexistence of lmp-like and gmp-like leukemia stem cells in acute myeloid leukemia. *Cancer cell*, 19(1):138–152, 2011.
- [13] Armin Attar. Changes in the cell surface markers during normal hematopoiesis: a guide to cell isolation. *Global Journal of Hematology and Blood Transfusion*, 1(1):20–28, 2014.
- [14] PDQ® Adult Treatment Editorial Board. PDQ® acute myeloid leukemia treatment. Online, 2023. Bethesda, MD: National Cancer Institute. Updated 01/18/2023. Available at: <https://www.cancer.gov/types/leukemia/hp/adult-aml-treatment-pdq>. [PMID: 26389432].
- [15] Elli Papaemmanuil, Hartmut Doehner, and Peter J Campbell. Genomic classification in acute myeloid leukemia. *The New England journal of medicine*, 375(9):900–901, 2016.
- [16] Erik Hulegårdh, Christer Nilsson, Vladimir Lazarevic, Hege Garelius, Petar Antunovic, Åsa Rangert Derolf, Lars Möllgård, Bertil Uggla, Lovisa Wennström, Anders Wahlin, et al. Characterization and prognostic features of secondary acute myeloid leukemia in a population-based setting: A report from the swedish acute leukemia registry. *American journal of hematology*, 90(3):208–214, 2015.
- [17] JM Bennett, D Catovsky, Marie-Therese Daniel, and G Flandrin. Galton dag, gralnick hr, sultan c: Proposals for the classification of the acute leukaemias. *Br J Haematol*, 33:451, 1976.
- [18] Peter B. Neame, Praniti Soamboonsrup, George P. Browman, Ralph M. Meyer, Ann Benger, W. Edwin C. Wilson, Irwin R. Walker, Niloufer Saeed, and John A. McBride. Classifying acute leukemia by immunophenotyping: A combined fab-immunologic classification of aml. *Blood*, 68(6):1355–1362, 1986.
- [19] Hartmut Döhner, Elihu Estey, David Grimwade, Sergio Amadori, Frederick R Appelbaum, Thomas Büchner, Hervé Dombret, Benjamin L Ebert, Pierre Fenaux, Richard A Larson, et al. Diagnosis and management of aml in adults: 2017 eln recommendations from an international expert panel. *Blood, The Journal of the American Society of Hematology*, 129(4):424–447, 2017.
- [20] Sandra Huber, Constance Baer, Stephan Hutter, Frank Dicker, Manja Meggendorfer, Christian Pohlkamp, Wolfgang Kern, Torsten Haferlach, Torsten Haferlach, and Gregor Hoermann. Aml classification in the year 2023: How to avoid a babylonian confusion of languages. *Leukemia*, pages 1–8, 04 2023.
- [21] Joseph D Khoury, Eric Solary, Oussama Abla, Yasmine Akkari, Rita Alaggio, Jane F Apperley, Rafael Bejar, Emilio Berti, Lambert Busque, John KC Chan, et al. The 5th

- edition of the world health organization classification of haematolymphoid tumours: myeloid and histiocytic/dendritic neoplasms. *Leukemia*, 36(7):1703–1719, 2022.
- [22] Rama Al Hamed, Abdul Hamid Bazarbachi, Florent Malard, Jean-Luc Harousseau, and Mohamad Mohty. Current status of autologous stem cell transplantation for multiple myeloma. *Blood cancer journal*, 9(4):44, 2019.
- [23] Andy GX Zeng, Suraj Bansal, Liqing Jin, Amanda Mitchell, Weihsu Claire Chen, Hussein A Abbas, Michelle Chan-Seng-Yue, Veronique Voisin, Peter van Galen, Anne Tierens, et al. A cellular hierarchy framework for understanding heterogeneity and predicting drug response in acute myeloid leukemia. *Nature medicine*, 28(6):1212–1223, 2022.
- [24] Aysun Adan, Günel Alizada, Yağmur Kiraz, Yusuf Baran, and Ayten Nalbant. Flow cytometry: basic principles and applications. *Critical reviews in biotechnology*, 37(2):163–176, 2017.
- [25] Swapnil Potdar, Aleksandr Ianevski, John Patrick Mpindi, Dmitrii Bychkov, Clément Fiere, Philipp Ianevski, Bhagwan Yadav, Krister Wennerberg, Tero Aittokallio, Olli Kallioniemi, et al. Breeze. *Bioinformatics*, 36(11):3602–3604, 2020.
- [26] Zuguang Gu and Daniel Hübschmann. Make interactive complex heatmaps in r. *Bioinformatics*, 38(5):1460–1462, 2022.